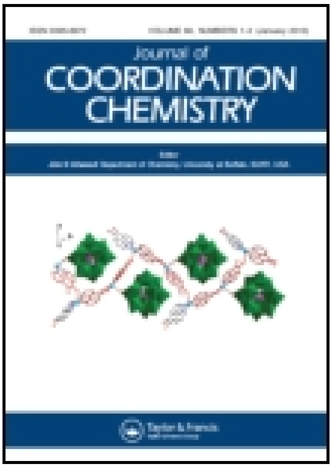

Journal of Coordination Chemistry
Publication details, including instructions for authors and subscription information:
http://www.tandfonline.com/loi/gcoo20

Three new mononuclear group 12 complexes with benzimidazole

Thaeny C. Amaral[a], Gustavo S.G. De Carvalho[b], Adilson D. Da Silva[b], Pedro P. Corbi[c], Norberto Masciocchi[d], Eduardo E. Castellano[e] & Alexandre Cuin[a]

[a] LQBin, Laboratório de Química BioInorgânica, Departamento de Química, Instituto de Ciências Exatas, Juiz de Fora, Brazil

[b] Departamento de Química, Instituto de Ciências Exatas, Juiz de Fora, Brazil

[c] Instituto de Química, Universidade Estadual de Campinas-UNICAMP, Campinas, Brazil

[d] Dipartimento di Scienza e Alta Tecnologia, Università degli Studi dell'Insubria, Como, Italy

[e] Instituto de Física, Universidade de São Paulo-USP, São Carlos, Brazil

To cite this article: Thaeny C. Amaral, Gustavo S.G. De Carvalho, Adilson D. Da Silva, Pedro P. Corbi, Norberto Masciocchi, Eduardo E. Castellano & Alexandre Cuin (2014) Three new mononuclear group 12 complexes with benzimidazole, Journal of Coordination Chemistry, 67:8, 1380-1391, DOI: 10.1080/00958972.2014.914179

To link to this article: http://dx.doi.org/10.1080/00958972.2014.914179

Journal of Coordination Chemistry, 2014
Vol. 67, No. 8, 1380–1391, http://dx.doi.org/10.1080/00958972.2014.914179

Three new mononuclear group 12 complexes with benzimidazole

THAENY C. AMARAL†, GUSTAVO S.G. DE CARVALHO‡, ADILSON D. DA SILVA‡, PEDRO P. CORBI§, NORBERTO MASCIOCCHI¶, EDUARDO E. CASTELLANO‖ and ALEXANDRE CUIN*†

†LQBin, Laboratório de Química BioInorgânica, Departamento de Química, Instituto de Ciências Exatas, Juiz de Fora, Brazil
‡Departamento de Química, Instituto de Ciências Exatas, Juiz de Fora, Brazil
§Instituto de Química, Universidade Estadual de Campinas-UNICAMP, Campinas, Brazil
¶Dipartimento di Scienza e Alta Tecnologia, Università degli Studi dell'Insubria, Como, Italy
‖Instituto de Física, Universidade de São Paulo-USP, São Carlos, Brazil

(*Received 12 November 2013; accepted 24 March 2014*)

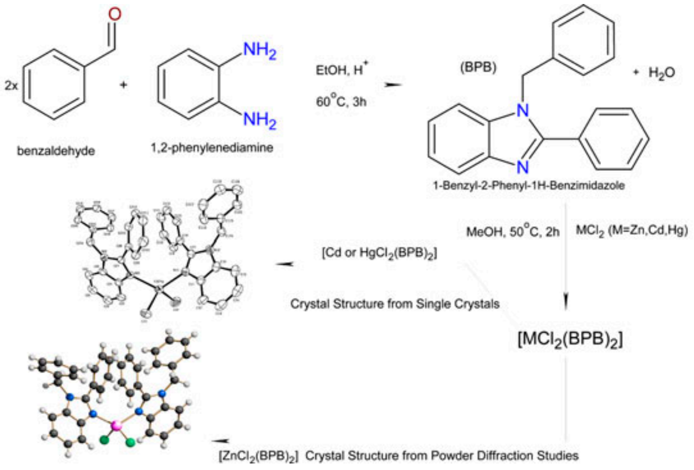

Three iso-structural Zn(II), Cd(II), and Hg(II) complexes with 1-benzyl-2-phenyl-1H-benzimidazole (BPB), ZnBPB, CdBPB, and HgBPB, respectively, were synthesized by reaction of the ligand with the corresponding metal chlorides in methanolic solutions. The complexes $[MCl_2(BPB)_2]$, where M = Zn(II), Cd(II), or Hg(II), were characterized by elemental analysis, ^{13}C, ^{1}H, and $[^{1}H–^{15}N]$ heteronuclear multiple bond coherence NMR measurements, and Raman spectroscopy. The structures of the cadmium and mercury complexes were solved by single-crystal X-ray diffraction, while the structure of the zinc complex was determined by X-ray powder diffraction. The three compounds crystallize in the triclinic system in *P-1* space group with the metal ions lying in a distorted tetrahedral environment. The zinc complex shows high luminescence in the solid state at room temperature.

Keywords: Zinc; Cadmium; Mercury; Powder diffraction; 1-Benzyl-2-phenyl-1H-benzimidazole

---

*Corresponding author. Email: alexandre.cuin@ufjf.edu.br

1. Introduction

Benzimidazoles are a class of organic compounds which possess extensive applications, especially in medicinal chemistry and a number of compounds containing a benzimidazole have been prepared and described with anti-inflammatory [1], anticancer [2], antimicrobial [3–5], antifungal [6], antiparasitic [7, 8], and antiviral activities [9]. Benzimidazole-based metal complexes with luminescent properties [10–13] are also known. In coordination chemistry, benzimidazoles are excellent *N*-donor ligands with formation of various metal complexes that exhibit different coordination numbers and geometries [14–16]. In this article, we report the synthesis, analytical, spectroscopic, and luminescence data of group 12 metal complexes with 1-benzyl-2-phenyl-1-benzimidazole (BPB, chart 1). Crystal structures of three complexes obtained by single crystal and less conventional powder diffraction methods are reported.

2. Experimental

2.1. *Physical techniques and materials*

All reagents and solvents for syntheses and spectroscopic studies were purchased from Sigma-Aldrich and used without purification. All spectra were recorded on Bruker spectrometers. The ^{13}C NMR spectrum of BFB was recorded on an Avance II instrument operating at 62.5 MHz while HgBFB and CdBFB ^{13}C NMR spectra were recorded on an Avance 600 instrument operating at 150 MHz, and finally ZnBFB ^{13}C NMR spectrum was obtained on an Avance 500 instrument operating at 125 MHz. The ^{13}C NMR chemical shifts were referenced to an internal standard (tetramethylsilane – TMS). The ^{1}H and ^{15}N NMR spectra were obtained on an Avance III 400 MHz (9.395T) instrument, specifically the ^{15}N NMR spectra

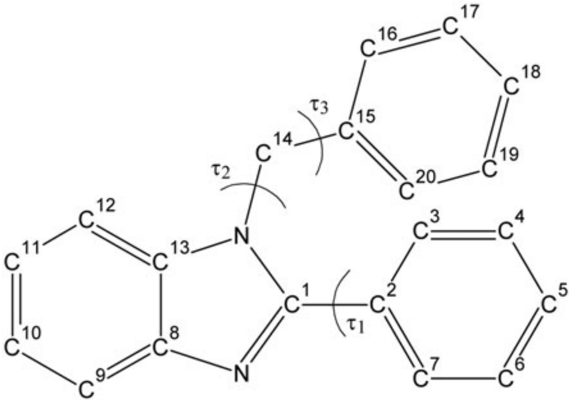

Chart 1. Sketch of BPB molecule. Carbon atoms are numbered and hydrogens are omitted for clarity. The torsion angles refined in the powder diffraction analysis of the ZnBPB complex are indicated as $\tau1$, $\tau2$, and $\tau3$.

were acquired indirectly [^1H–^{15}N] by heteronuclear multiple bond coherence technique (HMBC) using a 5 mm probe and a temperature of 298 K. The ^{15}N NMR spectra (^1H–^{15}N HMBC) were obtained at 40.54 MHz. Samples were prepared in deuterated chloroform solutions ($CDCl_3$) and the chemical shifts are given relative to TMS. The Raman spectra were recorded on a Bruker spectrophotometer model RFS 100 equipped with Nd^{3+}/YAG laser at 1064 nm and with 1.0 cm^{-1} resolution. The excitation and emission spectra of complexes were obtained using a fluorescence master system PTI spectrofluorometer.

2.2. *Syntheses*

BPB: benzaldehyde (19.62 mM, 2.0 mL) was added to an ethanolic solution containing 10 mL of 1,2-phenylenediamine (1.06 g, 9.81 mM). After 10 min, 0.50 mL of HCl (0.10 M L^{-1}) was added and the final solution was stirred for 3 h at room temperature. A polycrystalline compound was obtained and collected by filtration, washed with cold ethanol, and dried in a desiccator with silica. The BFB can also be obtained using basic solution [17] or microwave radiation [18]. A feasible mechanism from Schiff bases to benzimidazoles was recently described [18, 19].

Complexes: the dichlorobis(1-benzyl-2-phenyl-1H-benzimidazole)cadmium(II) and dichlorobis(1-benzyl-2-phenyl-1H-benzimidazole)mercury(II) complexes (named CdBPB and HgBPB) were obtained by reaction of 1.0 mM of MCl_2 (M = Cd, Hg) with 2.0 mM of BPB in methanolic solution under stirring at 50 °C for 2 h. The solid compounds obtained were collected by filtration. Crystals suitable for single-crystal X-ray analyses were obtained from the supernatants which were left to stand for a few days. The dichlorobis(1-benzyl-2-phenyl-1H-benzimidazole)zinc(II) complex (ZnBPB) was prepared in the same way as CdBPB and HgBPB. However, only a polycrystalline powder was obtained. The solid was collected by filtration and dried in a desiccator with silica before characterization.

2.3. *Single X-ray data collection and structure determination*

Single crystals of CdBPB and HgBPB were measured on an Enraf-Nonius Kappa-CCD diffractometer with graphite monochromated MoKα ($\lambda = 0.71073$ Å) radiation. Data were collected at room temperature up to 52° in 2θ and final unit cell parameters were based on all reflections. Data collections were made using the *COLLECT* program [20]. Integration and scaling of the reflections were performed with the HKL Denzo–Scalepack system of programs [21]. Absorption corrections were carried out using the RefDelF procedure [22]. The structure was solved by direct methods with *SHELXS-97* [23]. The model was refined by full-matrix least squares on F^2 using *SHELXL-97* [24]. All hydrogens were stereochemically positioned and refined with the riding model.

2.4. *Structural analysis of ZnBPB by X-ray powder diffraction data*

The polycrystalline ZnBPB complex was gently ground in an agate mortar. The powder was deposited in a sample holder equipped with a silicon zero-background plate. The diffraction data were collected by overnight scans in the 2θ range of 3°–105° with steps of 0.02° using a Bruker AXS D8 Advance diffractometer equipped with Ni-filtered CuKα radiation ($\lambda = 1.5418$ Å) and Lynxeye linear position-sensitive detector. The following optics were set up: primary beam Soller slits as 2.3°, fixed divergence slit as 0.5°, and receiving slit as 8 mm. The generator was set at 40 kV and 40 mA. Standard peak search, followed by indexing through the single-value decomposition approach implemented in TOPAS [25] allowed detection of the approximate triclinic unit cell parameters. Density considerations suggested $Z = 2$ and the space group *P-1* was chosen. Structure solution was performed by the simulated annealing technique implemented in TOPAS. The rigid body for BPB described as cartesian coordinates was employed where translations, rotations, and torsion angles (see chart 1) were left free. Zinc and chloride ions were freely floating. Final refinements were carried out by the Rietveld method maintaining the rigid body introduced at the solution stage. The background was modeled by a Chebyshev polynomial function and peak width anisotropy was described by a spherical harmonics model. An isotropic thermal parameter was assigned to the metal (B_M) and refined; lighter atoms were given a $B_{iso} = B_M + 2.0\,\text{Å}^2$ thermal parameter. The final Rietveld refinement plot is supplied as figure 1.

3. Results and discussion

3.1. *Elemental analyses*

Elemental analyses and complementary analytical data for free BPB and its Zn(II), Cd(II), and Hg(II) complexes are presented in table 1. The experimental data match with the molar composition $[MCl_2(BPB)_2]$.

3.2. *Spectroscopic studies*

BPB and its Zn(II), Cd(II), and Hg(II) complexes show quite similar Raman spectra and all spectra are reported in Supplementary material. The most important bands and the assignments are described in table 2. The combination band between νC=N and the

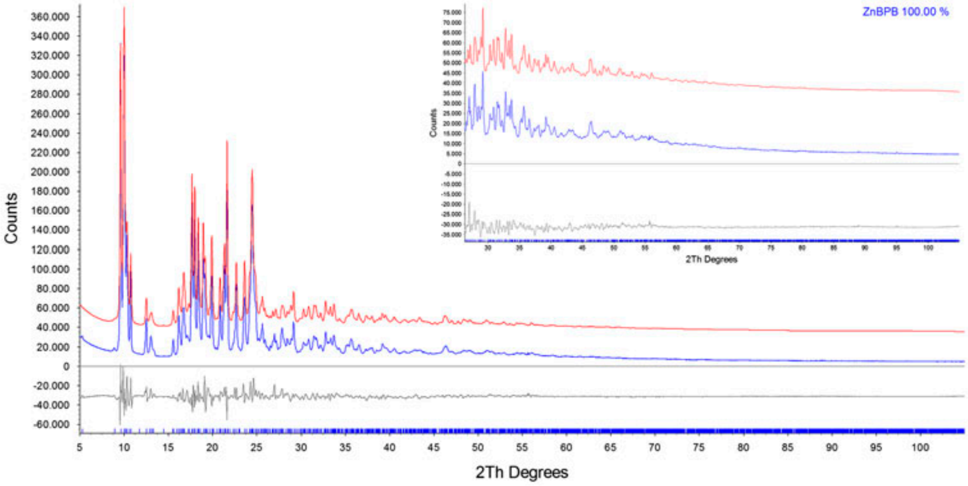

Figure 1. Final Rietveld refinement plot for ZnBPB with difference plot and peak markers at the bottom. The insert shows the high angle region at a magnified scale (5x).

Table 1. Analytical data for BPB and its Zn(II), Cd(II), and Hg(II) complexes.

Compound	Formula (MW, gM^{-1})	Yield (%)	Color	MP (°C)	Analytical data found (Calcd), % C	H	N
BPB [17]	$C_{20}H_{16}N_2$ (284.3)	90	Yellow	118	84.4 (84.5)	5.55 (5.67)	9.89 (9.85)
ZnBPB	$[Zn(C_{20}H_{16}N_2)_2Cl_2]$ (705.03)	77	Colorless	283	67.9 (68.1)	4.57 (4.57)	7.90 (7.95)
CdBPB	$[Cd(C_{20}H_{16}N_2)_2Cl_2]$ (752.03)	70	Colorless	230	64.0 (63.9)	4.59 (4.29)	7.40 (7.45)
HgBPB	$[Hg(C_{20}H_{16}N_2)_2Cl_2]$ (840.20)	84	Colorless	201	57.1 (57.2)	3.82 (3.84)	6.67 (6.67)

Table 2. Raman resonances of BPB and its group 12 metal complexes.

BPB	ZnBPB	CdBPB	HgBPB	Assignment
1603*s*	1606*s*	1607*s*	1606*s*	νC=N + νCC_{arom}
1515*s*	1519*s*	1523*s*	1519*s*	νC=N + νCC_{arom}
1442*s*	1455*s*	1455*s*	1454*s*	νCC_{arom}
1004*s*	1002*s*	1004*s*	1002*s*	νC–N
	165*w*	164*w*	159*w*	νM–Cl/νM–N

Note: *s* = strong, *w* = weak.

aromatic carbon bonds νCC_{arom} is observed at 1603 cm^{-1} for BPB [26]. The same combined band is observed at 1606–1607 cm^{-1} for Zn(II), Cd(II), and Hg(II) complexes showing a small and well-known [27] displacement when BPB is coordinated to metal ions. Beyond 250 cm^{-1}, free BPB shows two weak bands at 210 and 188 cm^{-1}. The Raman spectra of MCl_2 (M=Zn, Cd, and Hg) were also measured: for $ZnCl_2$, bands at 130 and 91 cm^{-1} are observed, whereas $CdCl_2$ and $HgCl_2$ show resonances at 162 and 121 cm^{-1}. Weak bands are observed at 213, 198, and 165 cm^{-1} for ZnBPB and 215, 196, and 164 cm^{-1} for CdBPB. For HgBPB, it is also possible to observe weak bands at 213 and 192 cm^{-1} while stronger bands appear at 252 and 159 cm^{-1}. Following previous reports, we assign the resonances of the M–Cl or M–N bond stretch where M = Zn(II), Cd(II), and Hg(II) at 165 cm^{-1}, 164 cm^{-1} [28], and 159 cm^{-1} [29], respectively.

The observed chemical shifts and the respective assignments of ^{13}C and ^{1}H data for BPB are described in table 3. The ^{13}C, ^{1}H, and ^{15}N NMR spectra of BPB and the complexes are very similar and only NMR data for BFB are shown in table 3. However, the ^{1}H, ^{13}C, and $[^{1}H–^{15}N]$ spectra of BFB and its Zn(II), Cd(II), and Hg(II) complexes are available as Supplementary material. The carbon numbering scheme in chart 1 is used to simplify the NMR assignments and discussion. The C14 (the only $–CH_2–$ present in BPB) appears at 47.9 ppm in all ^{13}C NMR spectra. The chemical shift of the carbon of –N=C–(C1) is observed at 153.8 ppm for BPB and for the three complexes. There are a few peaks in the 110–131 ppm range which are attributed to carbons present in the three phenyl rings (C3–C7, C9–C12, and C16–C20) and four other peaks at 136.3, 136.4, 137.4, and 143.1 ppm which are related to the C15, C2, C13, and C8, respectively. In the same way, peaks in all ^{1}H spectra are similar. The ^{15}N chemical shift for BPB was indirectly detected by $[^{1}H–^{15}N]$ HMBC experiments. Only one signal assigned to nitrogen bonded to C14 was found at 148 ppm coupling with hydrogens of $–CH_2–$ (two-bond correlation). For Zn(II), Cd(II), and Hg(II) complexes, the same resonance falls at 149 ppm showing a minimal shift. Multiple-bond

Table 3. ^{13}C and ^{1}H NMR data of free BPB.

^{13}C NMR data			
–CH$_2$–, C14	C3,C4,C5,C6,C7; C9,C10,C11,C12; C16,C17,C18,C19,C20	N=C, C1	C15, C2, C13, C8
47.9	111.5; 119.7; 122.7; 123.1; 126.5; 127.9; 129.2; 129.5; 130.6	153.7	136.3; 137.3; 143.1
^{1}H NMR data			
–CH$_2$–	Aromatic hydrogen atoms		
5.58(2)*s*	6.99(2)*d*; 7.25(5)*m*; 7.46 and 7.53(4)*m*; 7.73(3)*m*		

Note: *s*, singlet; *d*, doublet; *m*, multiplet. The numbers in parentheses refer to the number of protons as derived from integration of the signals.

correlation of this nitrogen with hydrogen bonded to C12 (aromatic) was not observed. Also, possible interactions of the N of –N=C– with hydrogens of phenyl rings which required three-bond correlation were not observed.

3.3. *Crystal structure studies*

The structures of the three molecular compounds have been derived from single-crystal (CdBPB and HgBPB) or powder (ZnBPB) X-ray diffraction analyses (crystallographic data are supplied in table 4). The latter method for specimens of moderate complexity can afford interesting crystallochemical information (stoichiometry, crystal packing, and conformation) at the expenses of relatively high idealization. In this case, as reported in the Experimental section, extensive use of (partially flexible) rigid bodies does not allow discussion of relevant intramolecular features but only a cross-comparison of ZnBPB with the Cd and Hg analogs. Accordingly, the most relevant bond distances, angles, and torsions of the ZnBPB, CdBPB, and HgBPB complexes are listed in tables 5 and 6 to a different number of significant digits (see esd's – estimated standard deviations).

Crystals of the three species are triclinic, space group *P-1*, and contain independent molecules packed by weak van der Waals interactions, since neither specifically polar moieties nor acidic hydrogens can be found on their periphery. However, a few weak H···Cl and H···C$_{\text{aromatic}}$ intermolecular interactions can be distinctly evidenced in all cases.

The three MBPB structures (M = Zn, Cd, Hg) can be considered isomorphous, although lattice constants and particularly the interaxial angles appear significantly different to a level that the originally collected powder diffraction trace of ZnBPB could *by no means* be associated with those computed from the already available single-crystal structures of CdBPB and HgBPB.

The molecular structures of CdBPB and HgBPB complexes are shown as ORTEP 3 [30] plots in figure 2((a) and (b), respectively) and are nearly undistinguishable at the drawn resolution. At variance, the molecule of ZnBPB drawn by SCHAKAL [31] appears in a nearly iso-oriented way in panel *c* of figure 2. In figure 3, the overall crystal packing of ZnBPB is presented which to some extent also represents those of CdBPB and HgBPB.

A number of torsion angles defining the ligand conformations for free BPB, Zn(II), Cd (II), and Hg(II) complexes and similar compounds [17, 32, 33] are reported in table 6. The molecular structures of similar Cd(II) and Hg(II) complexes were very recently reported by Manjunatha *et al.* [32] soon after the crystal structure of free BPB appeared, in 2009 [17]. As expected, slight changes in the conformation of the ligands were observed.

Table 4. Crystallographic data of ZnBPB, CdBPB, and HgBPB complexes.

	ZnBPB	CdBPB	HgBPB
CCDC number	966369	966370	966371
Empirical formula	$C_{40}H_{32}Cl_2N_4Zn$	$C_{40}H_{32}CdCl_2N_4$	$C_{40}H_{32}Cl_2HgN_4$
Formula weight	704.97	752.00	840.19
T (K)	296(2)	296(2)	296(2)
Wavelength (Å)	1.5418	0.71073	0.71073
Crystal system	Triclinic	Triclinic	Triclinic
Space group	*P-1*	*P-1*	*P-1*
Cell parameters			
a (Å)	10.9295(6)	10.6138(3)	10.6092(3)
b (Å)	10.2607(6)	10.8766(4)	10.8694(4)
c (Å)	18.725(1)	17.5400(6)	17.5869(6)
α (°)	87.321(6)	79.851(2)	80.050(2)
β (°)	64.346(4)	74.691(2)	74.690(2)
γ (°)	65.084(4)	62.491(2)	62.401(2)
Z	2	2	2
Volume (Å^3)	1693.0(2)	1728.71(1)	1730.47(1)
D_{Calcd} (g/cm^3)	1.383	1.445	1.612
μ (mm^{-1})	2.73	0.821	4.636
F (0 0 0)	728	764	828
Number of parameters	61	424	424
R, *wR*	0.028, 0.081[a]	0.0772, 0.194	0.0557, 0.131
$\Delta\rho_{\mathrm{min}}$, $\Delta\rho_{\mathrm{max}}$ (eA^3)	–	−0.67, 3.00	−1.21, 1.80
Goodness-on-fit (GOF)	10.68 [a]	1.011	1.069

[a] Profile values for powder diffraction study.

Table 5. Chemically relevant bond distances (Å) and angles (°) for ZnBPB, CdBPB, and HgBPB.

	ZnBPB	CdBPB	HgBPB
M–Cl	2.269(1)/2.320(1)	2.437(2)/2.449(2)	2.450(2)/2.472(2)
M–N	2.041(9)/2.050(8)	2.240(4)/2.289(4)	2.252(4)/2.266(4)
Cl–M–Cl	115.81(5)	114.77(7)	116.18(7)
N–M–N	120.02(4)	119.13(14)	119.03(16)

Table 6. Torsion angles of BPB and its group 12 complexes and related compounds.

	τ_1	τ_2	τ_3	τ_4
BPB [17]	+31.28	−101.79	+12.91	–
ZnBPB	+44.93	−111.60	+34.30	25.20
	+42.86	−100.78	+19.67	33.43
CdBPB	+45.75	−101.61	+24.88	+28.79
	+44.34	−103.70	+25.87	+31.35
HgBPB	+45.09	−103.07	+25.64	+27.15
	+46.21	−102.42	+26.28	+32.27
mbmpi	+35.68	−113.65	+17.40	–
Cdmbmpi [32]	+53.14	−132.38	+49.12	+40.85
Hgmbmpi [32]	+53.47	−133.21	+49.69	+41.57

Note: τ_4 was defined as torsion angle formed by N–M–N–C, where M is the metal ion and C is the carbon atom of –N = C–N– group and τ_1, τ_2, and τ_3 were defined according to chart 1.

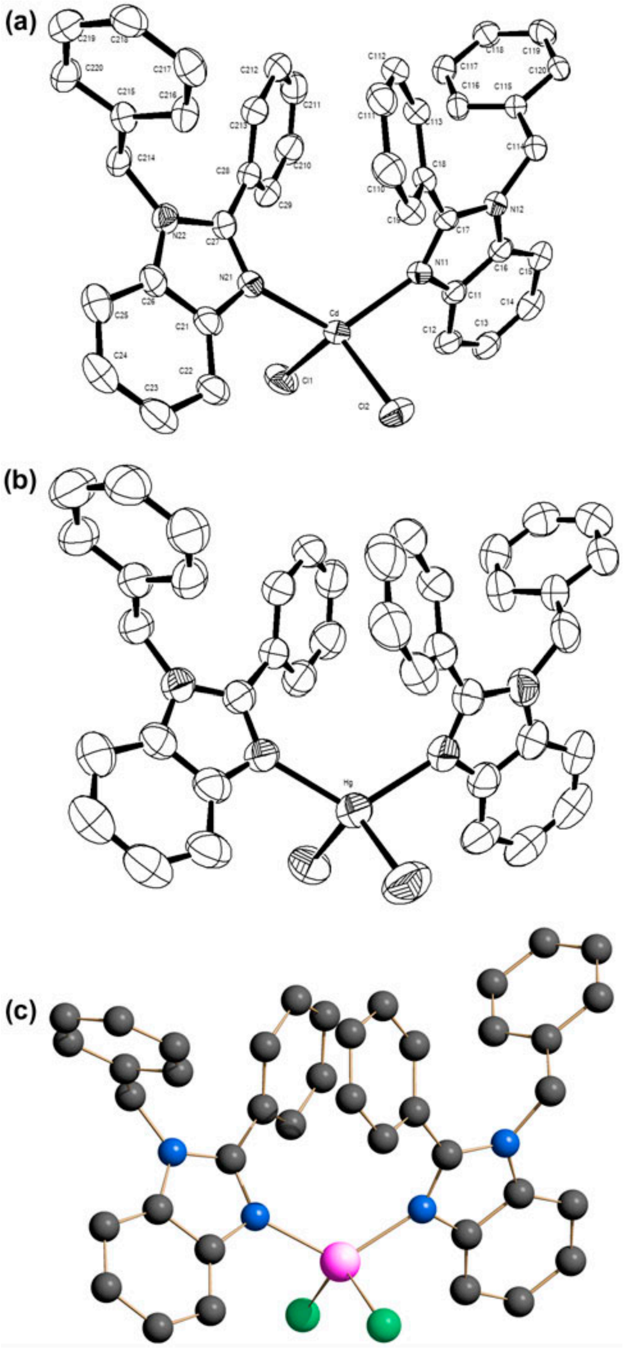

Figure 2. ORTEP views of CdBPB ((a) with atom labeling) and HgBPB (b) molecules. Hydrogens are not included in the drawings. (c) SCHAKAL plot for the ZnBPB complex, iso-oriented with (a) and (b). Zinc ion is in pink while chlorine and nitrogens are green and blue, respectively (see http://dx.doi.org/10.1080/00958972.2014.914179 for color version).

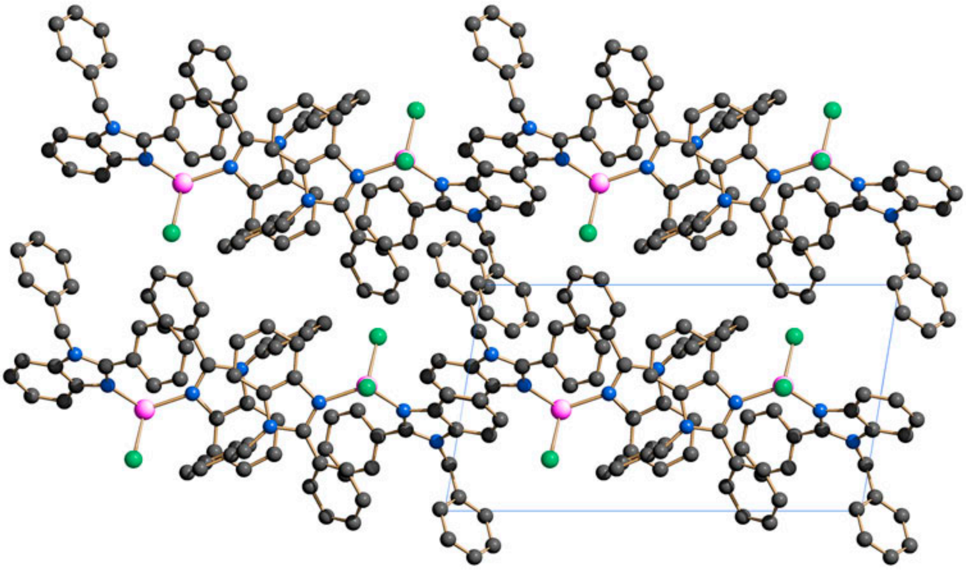

Figure 3. The crystal packing of ZnBPB viewed down (1 0 0). Horizontal axis is *c*.

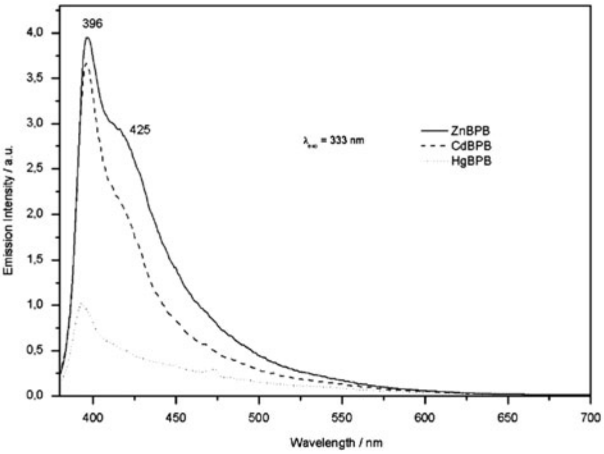

Figure 4. Solid-state emission of three complexes at room temperature using wavelength of excitation at 333 nm.

3.4. *Photoluminescence behavior*

Preliminary solid-state photoluminescence properties of the three complexes were studied at room temperature (298 K). The emission spectra of complexes were obtained by exciting the samples using λ_{exc} 333, 355, and 368 nm. ZnBPB is the most fluorescent complex while CdBPB and HgBPB are progressively less luminescent. In particular, when $\lambda_{exc} = 333$ nm was used (see figure 4), ZnBPB has a maximum emission at 396 nm with a shoulder

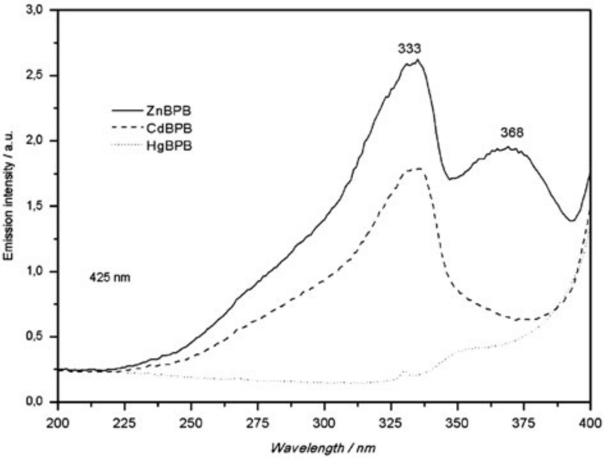

Figure 5. Emission spectra of the three complexes. Excitation has been observed between 200 and 400 nm with the fluorescence detector fixed at 425 nm.

centered near 425 nm; the same behavior was found for CdBPB but the shoulder near 425 nm becomes less perceptible. The photoluminescence behavior of BFB complexes is similar to luminescence properties of related compounds [34, 35].

Interestingly, when $\lambda_{exc} = 355$ or 368 nm were used, ZnBPB shows only one strong emission peak (at 425 nm) while the overall emission of HgBPB and CdBPB are significantly quenched. All observed peaks can be attributed to $\pi \rightarrow \pi^*$ intra-ligand or ligand-to-metal charge transfer mechanisms [36]. The excitation spectra of the three compounds obtained from 200 to 400 nm with fluorescence detection fixed at 425 nm are quite different (figure 5). The ZnBPB complex shows high fluorescence when considering $\lambda_{exc} = 333$ and 368 nm, whereas CdBPB only manifests the emission at $\lambda_{exc} = 333$ nm.

4. Conclusion

Three mononuclear $[MCl_2(BPB)_2]$ complexes (M = Zn(II), Cd(II), and Hg(II)) were obtained and characterized by analytical and spectroscopic measurements. Their structures determined by X-ray crystallography show that the ZnBPB, CdBPB, and HgBPB complexes are iso-structural with the metal ions lying in a distorted tetrahedral environment. The structure of the zinc complex was determined and refined from laboratory powder diffraction data *only* and as expected the quality of the structural model determined therefrom is much lower than from conventional single-crystal diffraction analysis. In the absence of single crystals of suitable size and quality, powder diffraction study discloses *otherwise inaccessible* structural information. All three complexes are luminescent; the higher quantum yields of ZnBPB make it a potentially useful photoactive material.

Supplementary material

Crystal data, fractional atomic coordinates, and displacement parameters of structures described in this article are supplied in standard CIFs deposited in the Cambridge

Crystallographic Data Center (966369, 966370, and 96671). The data can be obtained free of charge at http://www.ccdc.cam.ac.uk/conts/retrieving.html [or from Cambridge Crystallographic Data Center (CCDC), 12 Union Road, Cambridge CB2 1EZ, UK; Fax: +44 (0) 1223-336033; E-mail: deposit@ccdc.cam.ac.uk]. Also, complete set of Raman spectra and ^{1}H, ^{13}C, and [^{1}H–^{15}N] NMR spectra of BFB and its complexes are available as Supplementary material.

Funding

This work was supported by grants from FAPEMIG – Fundação de Amparo à Pesquisa do Estado de Minas Gerais (CEX-APQ-00256/11), CNPq – Conselho Nacional de Desenvolvimento Científico e Tecnológico (240094/2012-3 fellowship for Alexandre Cuin) and by FAPESP (Fundação de Amparo à Pesquisa do Estado de São Paulo – Grant # 2012/08230-2). The courtesy of Dr Angelo Maspero (University of Insubria) and Luca Nardo (University of Milano Bicocca) is heartily acknowledged.

Supplemental data

Supplemental data for this article can be accessed here http://dx.doi.org/10.1080/00958972.2014.914179

References

[1] S.M. Sondhi, R. Rani, J. Singh, P. Roy, S.K. Agarwal, A.K. Saxena. *Bioorg. Med. Chem. Lett.*, **20**, 2306 (2010).
[2] M. Andrzejewska, L. Yepez-Mulia, R. Cedillo-Rivera, A. Tapia, L. Vilpo, J. Vilpo, Z. Kazimierczuk. *Eur. J. Med. Chem.*, **37**, 973 (2002).
[3] A. Ünal, B. Eren. *Spectrochim. Acta A-M*, **114**, 129 (2013).
[4] K.F. Ansari, C. Lal. *Eur. J. Med. Chem.*, **44**, 4028 (2009).
[5] D.V. LaBarbera, E.B. Skibo. *Bioorg. Med. Chem.*, **13**, 387 (2005).
[6] H. Küçükbay, R. Durmaz, E. Orhan, S. Günal. *Farmaco*, **58**, 431 (2003).
[7] G. Navarrete-Vázquez, R. Cedillo, A. Hernández-Campos, L. Yépez, F. Hernández-Luis, J. Valdez, R. Morales, R. Cortés, M. Hernández, R. Castillo. *Bioorg. Med. Chem. Lett.*, **11**, 187 (2001).
[8] V.Z. Mota, G.S.G. Carvalho, A.D. Silva, L.A. Sodre-Costa, P.A. Machado, E.S. Coimbra, C.V. Ferreira, S.M. Shishido, A. Cuin. *BioMetals*, **27**, 183 (2014).
[9] J. Cheng, J. Xie, X. Luo. *Bioorg. Med. Chem. Lett.*, **15**, 267 (2005).
[10] H. Nozary, C. Piguet, P. Tissot, G. Bernardinelli, J.C.G. Bünzli, R. Deschenaux, D. Guillon. *J. Am. Chem. Soc.*, **120**, 12274 (1998).
[11] M. Elhabiri, R. Scopelliti, J.C.G. Bünzli, C. Piguet. *J. Am. Chem. Soc.*, **121**, 10747 (1999).
[12] G. Muller, J.C.G. Bünzli, K.J. Schenk, C. Piguet, G. Hopfgartner. *Inorg. Chem.*, **40**, 2642 (2001).
[13] E. Terazzi, S. Torelli, G. Bernardinelli, J. Rivera, J. Benech, C. Bourgogne, B. Donnio, D. Guillon, D. Imbert, J.C.G. Bünzli, A. Pinto, D. Jeannerat, C. Piguet. *J. Am. Chem. Soc.*, **127**, 888 (2005).
[14] D. Sarkar, A.K. Pramanik, T.K. Mondal. *Spectrochim. Acta A-M*, **115**, 421 (2013).
[15] Q.X. Liu, Q. Wei, X.J. Zhao, H. Wang, S.J. Li, X.G. Wang. *Dalton Trans.*, 5902 (2013).
[16] X.L. Wang, L.L. Hou, J.W. Zhang, G.C. Liu, H.Y. Lin. *Polyhedron*, **61**, 65 (2013).
[17] L. Kong. *Acta Crystallogr., Sect. E*, **E65**, o316 (2009).
[18] S. Perumal, S. Mariappan, S. Selvaraj. *Arkivoc,* VIII, 46–51 (2004).
[19] J.H. Hey, Y.X. Zhi, Y.Z. Zhi, J. Li, F.X. Zhang. *J. Coord. Chem.*, **66**, 1320 (2013).
[20] Enraf-Nonius. *COLLECT*, Nonius BV, Delft, The Netherlands (1997–2000).
[21] Z. Otwinowski, W. Minor, H.K.L. Denzo. In *Methods in Enzymology*, C.W. Carter Jr, R.M. Sweet (Eds), Vol. 276, Academic Press, New York, pp. 307 (1997).
[22] S. Parkin, B. Moezzi, H. Hope. *J. Appl. Cryst.*, **28**, 53 (1995).

[23] G.M. Sheldrick. *SHELXS-97, Program for Crystal Structure Refinement*, University of Gottingen, Germany (1997).

[24] G.M. Sheldrick. *SHELXS-97, Program for Crystal Structure Analysis*, University of Gottingen, Germany (1997).

[25] *TOPAS-R* (*Version 3.0*), Bruker AXS, Karlswhe, Germany (2005).

[26] V.Z. Mota, G.S.G. Carvalho, P.P. Corbi, F.R.G. Bergamini, A.L.B. Formiga, R. Diniz, M.C.R. Freitas, A.D. da Silva, A. Cuin. *Spectrochim. Acta A-M*, **99**, 110 (2012).

[27] B. Roopashree, V. Gayathri, H. Mukund. *J. Coord. Chem.*, **65**, 1354 (2012).

[28] G.A. Bowmaker, E. Fariati, S.I. Rahajoe, B.W. Skelton, A.H. White. *Z. Anorg. Allg. Chem.*, **637**, 1361 (2011).

[29] K.B. Nilsson, M. Maliarik, I. Persson, M. Sandstrom. *Dalton Trans.*, 2303 (2008).

[30] L.J. Farrugia. *J. Appl. Cryst.*, **30**, 565 (1997).

[31] E. Keller. *Chem. Unserer Zeit*, **20**, 178 (1986).

[32] M.N. Manjunatha, A.G. Dikundwar, K.R. Nagasundara. *Polyhedron*, **30**, 1299 (2011).

[33] H.W. Yang, F. Yue, S. Feng, J.D. Wang, H.A. Liu, H.M. Chen, K.B. Yu, Y. Huaxue. *Chin. J. Org. Chem.*, **24**, 792 (2004).

[34] B. Xiao, H. Hou, Y. Fany. *J. Coord. Chem.*, **62**, 1827 (2009).

[35] X.-Y. Hou, X. Wang, F. Fu, J.-J. Wang, L. Tang. *J. Coord. Chem.*, **66**, 3126 (2013).

[36] Y. Cui, Y. Yue, G. Qian, B. Chen. *Chem. Rev.*, **112**, 1126 (2012).